Eurographics Conference on Visualization (EuroVis) 2016
E. Bertini, N. Elmqvist, and T. Wischgoll
(Guest Editors)

Short Paper

Analysis of Error in Interpolation-Based Pathline Tracing

Jennifer Chandler[1], Roxana Bujack[1], and Kenneth I. Joy[1]

[1]University of California, Davis

Abstract

Chandler et al. [COJ15] presented interpolation-based pathline tracing as an alternative to numerical integration for advecting tracers in particle-based flow fields and showed that their method has lower error than a numerical integration-based method for particle tracing. We seek to understand the sources of the error in interpolation-based pathline tracing. We present a formal analysis of the theoretical bound on the error when advecting pathlines using this method. We characterize the error experimentally using characteristics of the flow field such as neighborhood change, flow divergence, and trajectory length. Understanding the sources of error in an advection method is important to know where there may be uncertainty in the resulting analysis. We find that for interpolation-based pathline tracing the error is closely related to the divergence in the flow field.

Categories and Subject Descriptors (according to ACM CCS): G.1.0 [Mathematics of Computing]: Numerical Analysis—Error Analysis G.1.0 [Mathematics of Computing]: Numerical Analysis—Interpolation

1. Introduction

Fluid simulations are used in many scientific application areas such as astrophysics, geology, and medicine. A fluid simulation can be classified as either Eulerian or Lagrangian. Eulerian fluid simulations evaluate physical quantities of the flow at a number of fixed reference points in the domain. This type of fluid simulation is very common, and analysis techniques for Eulerian simulations are well known. We focus on Lagrangian fluid simulations which evaluate the physical quantities of the flow on a set of moving reference points. Typically this takes the form of a particle-based fluid simulation. Particle-based flow fields have many advantages over vector field representations: it is easy to simulate moving obstacles and adjust for varying levels of detail in different regions of the flow.

Particle advection is the basis of many flow analysis techniques. Therefore, it is important to develop accurate algorithms for advecting particles in different types of flow fields. We analyze the error in the interpolation-based pathline tracing method of Chandler et al. [COJ15]. For a new method, it is important to understand sources of error as this affects the subsequent analysis of the data. Chandler et al. present a comparison of the average error of their method to Runge-Kutta 4/5 numerical integration. We examine the advection error compared to flow characteristics such as neighborhood change, flow divergence, and trajectory length and find that advection error is correlated with divergence in the flow. Additionally, we give a theoretical bound on the advection error using numerical analysis techniques. We examine the theoretical error for a single advection step and the accumulation of error over a pathline.

2. Background

Our work further analyzes and characterizes the advection error in the work of Chandler et al. [COJ15] on pathline tracing for particle-based flow fields. We review their method and present an overview of Smoothed Particle Hydrodynamics (SPH) fluid simulations.

2.1. Smoothed Particle Hydrodynamics

SPH is a particle-based fluid simulation method in which each particle carries physical quantities, such as density, pressure, and velocity, that define the flow field [GM77]. Each particle moves through the domain, and the output of the simulation is the location of each particle and the values of its physical quantities for every time step of the simulation. Each particle can be tracked across time steps so the simulation output forms a set of trajectories, or pathlines, describing the movement of the flow field over time.

In flow analysis, one often needs to sample a physical quantity at an arbitrary location in the domain. For an SPH simulation this is done by interpolation using a kernel weighting function W. Each simulation particle has an associated radius, called the smoothing length h, defining the region where it can be used for interpolation. Evaluating a quantity Q at location $\mathbf{P}$ takes the following form:

$$Q(\mathbf{P}) = \sum_i Q_i W(\|\mathbf{P} - \mathbf{P}_i\|, h_i). \tag{1}$$

2.2. Interpolation-based Pathline Tracing

Chandler et al. trace new pathlines in the flow field by interpolating the trajectories of the simulation particles. Their method uses the SPH kernel function to assign weights to neighboring particles surrounding the tracer particle to be advected. A neighboring particle is one whose smoothing length overlaps the advected location. After identifying the neighboring particles and assigning weights they use the following equation to advect the tracer particle $\mathbf{P}$:

$$\mathbf{P}(t_{j+1}) = \mathbf{P}(t_j) + \sum_i W_i(t_j)(\mathbf{P}_i(t_{j+1}) - \mathbf{P}_i(t_j)). \tag{2}$$

DOI: 10.2312/eurovisshort.20161152

After advecting the particle, they update the neighbors in the new time step to account for convergence and divergence and repeat the process for the remaining time steps. We analyze the error in this advection algorithm based on various characteristics of the flow field such as the neighborhood change, the flow divergence, and the magnitude of the reference tracer movement.

3. Related Work

In this section we focus on particle-based methods and error analysis for flow visualization. For an overview on flow visualization see Post et al. [PVH*03] and McLoughlin et al. [MLP*10].

In addition to Chandler et al.'s method, Agranovsky et al. also explore particle-interpolation-based methods. They advect particles in-situ and store the resulting trajectories as the simulation output [ACG*14]. They find that this representation is more efficient for post hoc analysis than a vector field representation. Bujack and Joy improve on this method of storing Lagrangian trajectories by using parameter curves to give a smoother representation of the trajectory and improve accuracy between stored time steps [BJ15]. Agranovsky et al. [AOGJ15] also use a multi-resolution Lagrangian representation to visualize path surfaces by interpolating the trajectories stored in a multi-resolution flow map.

Our work targets particle-based flow fields, specifically SPH simulations. Many visualization techniques for SPH simulations involve volume rendering of different physical quantities of the flow or column density, the integral of the density through the view direction. Price [Pri07], Fraedrich et al. [FAW10], and Reichl [RTW13] implement these types of techniques for SPH visualization. There has not been as much work in the area of extracting flow features from SPH simulations. Robinson [Rob09] presents a method for characterizing mixing behavior in SPH simulations using FTLE values. Cao [Cao13] uses FTLE values and rotation measures to visualize SPH simulations. Schindler et al. [SFBP09] extract vortex core lines in SPH simulations. Biddiscombe et al. [BGM07] combine 2D and 3D rendering for SPH and also show the trajectories of existing simulation particles.

Understanding sources of error is important for an accurate analysis of flow behavior. Chen et al. explore the error introduced by downsampling velocity fields in time by modeling the error as a Gaussian distribution [CBS15]. They use a forward and backward advection approach to minimize error between stored time steps. Lodha et al. visualize uncertainty in streamline tracing with different integration methods, representing potential error using glyphs and color maps [LPSW96]. Botchen et al. examine error introduced by acquiring flow data with Particle Image Velocimetry [BWE05]. They visualize the root mean square of the measurements using texture advection with blurring to represent uncertain areas. Lopez and Brodlie visualize the accuracy of particle advection using reintegration, velocity residuals, and global error from the integration method [LB98]. These works focus on understanding error in Eulerian flow fields; our work aims to characterize sources of error for interpolation-based advection in particle-based flow fields.

4. Theoretical Bound on Advection Error

In this section we give a theoretical bound on the error when tracing pathlines. Bujack and Joy [BJ15] have shown that this method is a special kind of numerical one-step integration method and have given a global error estimate for the case of linear interpolation on a regular grid. The main structure of our error is comparable, but instead of linear interpolation, we interpolate with the SPH smoothing kernel for an approximation of particle positions.

We approximate the path of an arbitrary location $\mathbf{P}$ using the particles $\mathbf{P}_i$ in its neighborhood $\|\mathbf{P}-\mathbf{P}_i\| \leq h_\mathbf{P}$ as described in Eq. 2. Using the flow map notation, this can be written as

$$P_{SPH}F^{t_j}_{t_{j-1}}(\mathbf{P}) = \quad F^{t_{j-1}}_{t_{j-1}}(\mathbf{P}) + \frac{\sum_{\mathbf{P}_i\in B_{h_\mathbf{P}}(\mathbf{P})} w_i (F^{t_j}_{t_{j-1}}(\mathbf{P}_i) - F^{t_{j-1}}_{t_{j-1}}(\mathbf{P}_i))}{\sum_{\mathbf{P}_i\in B_{h_\mathbf{P}}(\mathbf{P})} w_i}, \tag{3}$$

where P_{SPH} is the SPH interpolation, $h_\mathbf{P}$ is the smoothing length, $B_{h_\mathbf{P}}(\mathbf{P})$ is a ball with radius $h_\mathbf{P}$ around $\mathbf{P}$, and the weights w_i are computed using an SPH weighting kernel W. Applying the Taylor expansion with a value $t \in [t_{j-1}, t_j]$ reveals

$$P_{SPH}F^{t_j}_{t_{j-1}}(\mathbf{P}) = F^{t_{j-1}}_{t_{j-1}}(\mathbf{P}) + h_t \frac{\sum_{\mathbf{P}_i\in B_{h_\mathbf{P}}(\mathbf{P})} w_i \dot{F}^t_{t_{j-1}}(\mathbf{P}_i)}{\sum_{\mathbf{P}_i\in B_{h_\mathbf{P}}(\mathbf{P})} w_i}, \tag{4}$$

which means that the SPH interpolation has the form of a one-step integration method [Sch02, HH12].

The local truncation error T_j at particle $\mathbf{P}$ coincides with the interpolation error inferred by the SPH smoothing kernel. Using the multivariate Taylor expansion, [GL10], with $\zeta \in B_{h_\mathbf{P}}(\mathbf{P})$, we see

$$\begin{aligned}
T_j =& |P_{SPH}F^{t_j}_{t_{j-1}}(\mathbf{P}) - F^{t_j}_{t_{j-1}}(\mathbf{P})| \\
\overset{(3)}{=}& |F^{t_{j-1}}_{t_{j-1}}(\mathbf{P}) + \frac{\sum w_i (F^{t_j}_{t_{j-1}}(\mathbf{P}_i) - F^{t_{j-1}}_{t_{j-1}}(\mathbf{P}_i))}{\sum w_i} - F^{t_j}_{t_{j-1}}(\mathbf{P})| \\
\overset{\text{Taylor}}{=}& |F^{t_{j-1}}_{t_{j-1}}(\mathbf{P}) + \frac{\sum w_i (F^{t_j}_{t_{j-1}}(\mathbf{P}) - F^{t_{j-1}}_{t_{j-1}}(\mathbf{P}))}{\sum w_i} \\
& + \frac{\sum w_i (\mathbf{P}-\mathbf{P}_i)^T \nabla (F^{t_j}_{t_{j-1}}(\zeta) - F^{t_{j-1}}_{t_{j-1}}(\zeta))}{\sum w_i} - F^{t_j}_{t_{j-1}}(\mathbf{P})| \\
=& |\frac{\sum w_i (\mathbf{P}-\mathbf{P}_i)^T \nabla (F^{t_j}_{t_{j-1}}(\zeta) - F^{t_{j-1}}_{t_{j-1}}(\zeta))}{\sum w_i}| \\
\leq& \frac{\sum w_i \|\mathbf{P}-\mathbf{P}_i\|}{\sum w_i} \|\nabla (F^{t_j}_{t_{j-1}}(\zeta) - F^{t_{j-1}}_{t_{j-1}}(\zeta))\| \\
\leq& h_\mathbf{P} \|\nabla (F^{t_j}_{t_{j-1}}(\zeta) - F^{t_{j-1}}_{t_{j-1}}(\zeta))\|.
\end{aligned} \tag{5}$$

As is known from numerics of ordinary differential equations, the global truncation error E_j is related to local truncation error by

$$E_j \leq j \max_{i=1,\dots,j} T_i e^{L(t_j - t_0)} \tag{6}$$

with the Lipschitz constant L [Sch02, HH12]. That reveals

$$\begin{aligned}
E_j \overset{(5)}{\leq}& j \max_{i=1,\dots,j} \max_{\zeta\in\mathbb{R}^d} h_\mathbf{P} \|\nabla (F^{t_j}_{t_{j-1}}(\zeta) - F^{t_{j-1}}_{t_{j-1}}(\zeta))\| e^{L(t_j-t_0)} \\
\overset{\text{Taylor}}{\leq}& j \max_{i=1,\dots,j} \max_{\zeta\in\mathbb{R}^d} h_\mathbf{P} h_t \|\nabla \dot{F}^t_{t_{j-1}}(\zeta)\| e^{L(t_j-t_0)} \\
=& |t_j - t_0| h_\mathbf{P} \max_{i=1,\dots,j} \max_{\zeta\in\in\mathbb{R}^d} \|\nabla \dot{F}^t_{t_{j-1}}(\zeta)\| e^{L(t_j-t_0)}.
\end{aligned} \tag{7}$$

The latter estimate shows that the asymptotic behavior of the global truncation error for advecting a particle across a time interval only depends on the spatial resolution $h_\mathbf{P}$ and not the temporal

resolution h_t. This holds with the concept of a particle-based flow field storing trajectories that contain the exact start and end point for each particle, regardless of the number of time steps in between. It also holds with the experimental results shown by Chandler et al. [COJ15] in their skipping time steps test where the error does not increase when intermediate time steps are removed. We make use of the estimate (7) so that we can approximate the error for individual pathlines. We also explore this result further in Section 5. This error bound also supports the results shown by Agranovsky et al. [ACG*14] which demonstrate that storing particle trajectories rather than instantaneous velocities for the same number of time steps gives smaller advection error since advection using numerical integration has both spatial and temporal error.

5. Experimental Results

We present the results of characterizing the advection error compared to different flow field characteristics. The error is the distance from the advected particle to the simulation particle. We ran these tests on 3 different data sets. The first is a mixing simulation of a box filled with fluid and two co-rotating blades and has 2,097,152 particles. The second data set has 2,097,152 particles and simulates two fluid spheres hanging in the air that drop onto a planar surface. The particle movement is uniform until the impact when the fluid begins to splash around. The third data set has a heating mechanism at the bottom of a fluid-filled box with 124,768 particles. As the fluid is heated the bottom particles accelerate upward and cooler particles fall back down causing a high velocity jet in the center.

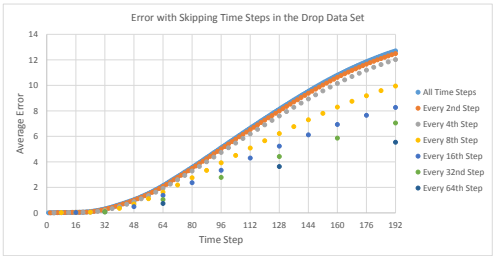

Figure 1: *This chart shows the average error at each time step when skipping time steps in between. For this test we use every n-th time step where n doubles for each successive run of the experiment. The results show that the error at a particular time step tends to be lower when fewer advection steps were taken to get there.*

5.1. Error with Skipping Time Steps

We extend the experiment by Chandler et al. to measure the error when skipping time steps to further analyze the results. We advect particles using every n-th time step and only measure the error at time steps that were used. See Figure 1. The results show that the error at a given time step tends to decrease when there were fewer advection steps taken between the initial and the given time step. This fits with the theoretical analysis which shows that the local truncation error (i.e. the error when advecting between two given time steps) is only dependent on the spatial resolution and not the temporal resolution. When advecting a particle using all time steps between the start and end point, the error tends to increase with each time step since it has both the local spatial error and the accumulated error from previous advection steps as shown in the global error approximation (Eq. 7). This result shows that interpolation-based pathline tracing is particularly useful when the goal is to analyze where particles travel after a long time period since only the time steps of interest are needed to get an accurate result, whereas with a numerical integration advection process the accuracy of the result is highly dependent on the temporal resolution.

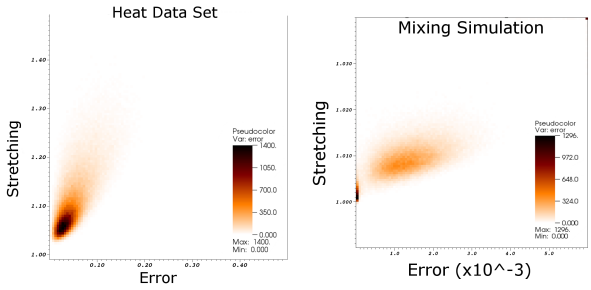

Figure 2: *These density plots show the relationship between the stretching value and the error in the heating and mixing data sets. After each advection step we re-seed the particles at the locations of the simulation particles so that we can measure the error after a single step for each time step in the simulation. A ratio of one means no stretching in the local neighborhood. In these charts higher error is correlated with higher stretching values.*

5.2. Error with Flow Divergence

For this experiment we observe the error with respect to the divergence in the flow field. We approximate divergence as a stretching value s, the ratio between the particle separation in the intial time step and the separation in the subsequent time step:

$$s = \max_{\mathbf{P}_i} \frac{|\mathbf{P}(t_{j+1}) - \mathbf{P}_i(t_{j+1})|}{|\mathbf{P}(t_j) - \mathbf{P}_i(t_j)|} \tag{8}$$

where $\mathbf{P}$ is the reference simulation particle where we have seeded a tracer particle, and the $\mathbf{P}_i$ are the neighboring particles. With this stretching metric a value of 1 means that there was no divergence in the flow field. Higher values indicate larger divergence in the neighborhood. In Figure 2 the results show that an increase in error is correlated with an increase in the stretching measurement.

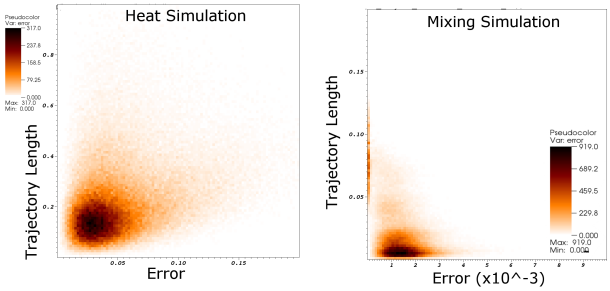

Figure 3: *These density plots compare the error with the length of the reference trajectory after a single advection step. After each advection step we re-seed the particles at the locations of the simulation particles so that we do not measure the effects of error accumulated due to multiple advection steps. We can see some correlation between the trajectory length and the error for the heat data set, but not much correlation for the mixing simulation.*

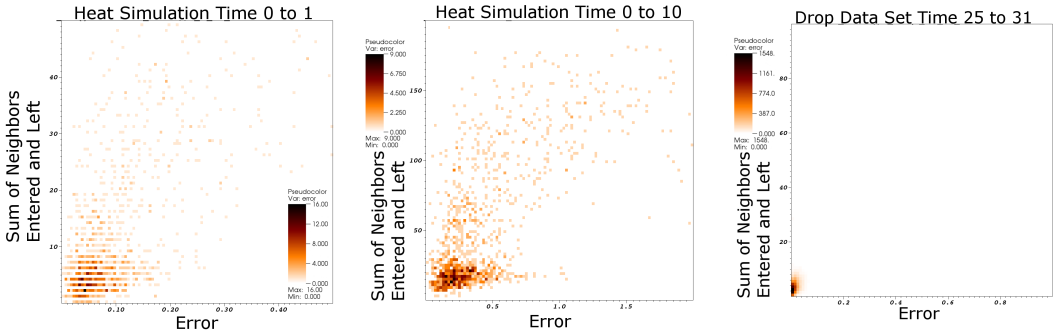

Figure 4: *These density plots show the results of comparing the neighborhood change to the average error. The neighborhood change is the sum of the particles that left the initial neighborhood and new particles that entered the neighborhood after the advection steps. The first chart shows the neighborhood change after a single advection step, while the second shows the neighborhood change after 10 advection steps in the heat data set. The third chart shows the neighborhood change in the drop data set for time steps 25 to 31 which is around the start of the fluid impact with the ground plane. The neighborhood change is much higher after many advection steps.*

5.3. Error with Trajectory Length

We examine the advection error compared to the length of the reference trajectory after a single advection step. We expected that longer trajectories would be correlated with higher error because particles that do not move much would have a lower probability of having a high error due to the interpolation process. We do see some correlation between trajectory length and error; however, it is not as strong as the correlation with stretching. This can be seen in Figure 3. The trajectory length is not a generally useful predictor of error since it is possible to have regions with fast moving particles that all move in the same direction. In this case the interpolation error would still be low, but the trajectory lengths would be long.

5.4. Error with Neighborhood Change

Interpolation-based pathline tracing updates the particle neighborhood after each advection step. Ideally, the particle neighborhood would stay the same; however, due to convergence and divergence, the neighborhood surrounding the tracer may change between time steps. We look at how many particles left the neighborhood and how many new ones entered in Figure 4. We see some correlation between neighborhood change and error. We look at the neighborhood change after multiple advection steps since particle neighborhoods change very little after a single advection step with a small time step length. After a certain point, if the entire neighborhood is different than the original one, then we do not expect this metric to show a strong correlation with error since the error can continue to grow in later time steps but neighborhood change is limited based on the number of initial neighbors. We expect that pathlines with higher error have very different neighborhoods than the initial ones since this indicates a high amount of divergence and convergence.

5.5. Relationship to Theoretical Error

To compute real values for the theoretical error, we must estimate the derivative $\nabla(F^{t_j}_{t_{j-1}}(\zeta_i)_l - F^{t_{j-1}}_{t_{j-1}}(\zeta_i)_l)$. This is not a trivial problem for scattered data. We approximated this value using moving least squares [Lev98]. We tried a first order and a second order approximation. The first order approximation gave smaller values than the observed error, while the second order approximation had a larger range of values. We found that there was no correlation between the

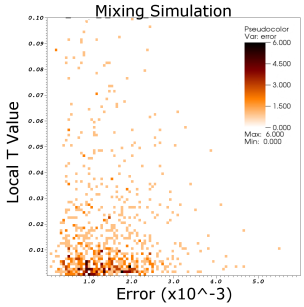

Figure 5: *This density plot shows the relationship between the T values approximated using moving least squares and the advection error in the mixing simulation. We do not see a correlation between the T values and the error using this approximation method.*

computed T values from the local truncation and the observed error from the advection results as shown in Figure 5. We believe that our theoretical error estimate is still a good bound on the error, but in order to use it in practice we need a better way to approximate the true value of the derivative in the local neighborhood.

6. Conclusion

We have shown a number of ways to characterize the advection error using interpolation-based pathline tracing. We found that the error is roughly correlated with divergence in the flow field. We showed that the error for advecting a pathline directly from the initial time step to a later time step is generally less than advecting it using all time steps in between. That can be seen, because the local truncation error is smaller than the global one according to our theoretical error analysis. Further, the stretching is correlated to the factor $\nabla(F^{t_j}_{t_{j-1}}(\zeta_i)_l - F^{t_{j-1}}_{t_{j-1}}(\zeta_i)_l)$ in Equation 5, which describes the change in the displacement vectors over time. Our theoretical bounds on the advection error can be used to identify which areas of the flow field are most prone to advection error. In future work we would like to investigate different ways to compute a better approximation of T so that we can visualize the theoretical error estimate for real data sets. We would like to further explore how the correlation between the stretching and advection error and the neighborhood change and advection error can be used to modify the interpolation-based pathline tracing method to reduce the error.

7. Acknowledgments

This work was supported in part by the National Science Foundation under contract IIS 1018097, NSF GRFP grant DGE-1148897, and the Office of Advanced Scientific Computing Research, Office of Science, of the U.S. Department of Energy under Contract No. DESC0007443 through the Scientific Discovery through Advanced Computing (SciDAC) programs Scalable Data Management, Analysis and Visualization Center (SDAV).

References

[ACG*14] AGRANOVSKY A., CAMP D., GARTH C., BETHEL E. W., JOY K. I., CHILDS H.: Improved post hoc flow analysis via Lagrangian representations. In *2014 IEEE 4th Symposium on Large Data Analysis and Visualization (LDAV)* (2014), IEEE, pp. 67–75. 2, 3

[AOGJ15] AGRANOVSKY A., OBERMAIER H., GARTH C., JOY K. I.: A multi-resolution interpolation scheme for pathline based Lagrangian flow representations. In *Proc. SPIE 9397, Visualization and Data Analysis 2015* (2015), vol. 9397, pp. 93970K–93970K–12. doi:10.1117/12.2083253. 2

[BGM07] BIDDISCOMBE J., GRAHAM D., MARUZEWSKI P.: Interactive visualization and exploration of SPH data. In *Proceedings of 2nd SPHERIC international workshop, Madrid (Spain)* (2007), Citeseer. 2

[BJ15] BUJACK R., JOY K. I.: Lagrangian representations of flow fields with parameter curves. In *2015 IEEE 5th Symposium on Large Data Analysis and Visualization (LDAV)* (2015), IEEE, pp. 41–48. 2

[BWE05] BOTCHEN R. P., WEISKOPF D., ERTL T.: Texture-based visualization of uncertainty in flow fields. In *IEEE Visualization, 2005* (oct 2005), pp. 647–654. 2

[Cao13] CAO W.: *Analysis Supported SPH Fluid Simulation*. Master's thesis, University of Houston, 2013. 2

[CBS15] CHEN C.-M., BISWAS A., SHEN H.-W.: Uncertainty modeling and error reduction for pathline computation in time-varying flow fields. In *2015 IEEE Pacific Visualization Symposium (PacificVis)* (April 2015), pp. 215–222. doi:10.1109/PACIFICVIS.2015.7156380. 2

[COJ15] CHANDLER J., OBERMAIER H., JOY K. I.: Interpolation-based pathline tracing in particle-based flow visualization. *IEEE Transactions on Visualization and Computer Graphics 21*, 1 (jan 2015), 68–80. doi:10.1109/TVCG.2014.2325043. 1, 3

[FAW10] FRAEDRICH R., AUER S., WESTERMANN R.: Efficient high-quality volume rendering of SPH data. *IEEE Transactions on Visualization and Computer Graphics 16*, 6 (nov-dec 2010), 1533–1540. 2

[GL10] GHORPADE S. R., LIMAYE B. V.: *A Course in Multivariable Calculus and Analysis*. Springer, New York, USA, 2010. 2

[GM77] GINGOLD R. A., MONAGHAN J. J.: Smoothed particle hydrodynamics-theory and application to non-spherical stars. *Monthly notices of the royal astronomical society 181* (1977), 375–389. 1

[HH12] HÄMMERLIN G., HOFFMANN K.-H.: *Numerical mathematics*. Springer Science & Business Media, 2012. 2

[LB98] LOPES A., BRODLIE K.: Accuracy in 3D particle tracing. In *Mathematical Visualization*. Springer, 1998, pp. 329–341. 2

[Lev98] LEVIN D.: The approximation power of moving least-squares. *The Mathematics of Computation 67*, 224 (Oct. 1998), 1517–1531. 4

[LPSW96] LODHA S., PANG A., SHEEHAN R., WITTENBRINK C.: UFLOW: Visualizing uncertainty in fluid flow. In *Proceedings of Visualization '96* (oct 1996), pp. 249–254. doi:10.1109/VISUAL.1996.568116. 2

[MLP*10] MCLOUGHLIN T., LARAMEE R. S., PEIKERT R., POST F. H., CHEN M.: Over two decades of integration-based, geometric flow visualization. *Computer Graphics Forum 29*, 6 (2010), 1807–1829. 2

[Pri07] PRICE D. J.: SPLASH: An interactive visualization tool for smoothed particle hydrodynamics simulations. *Publications of the Astronomical Society of Australia 24*, 3 (2007), 159–173. 2

[PVH*03] POST F. H., VROLIJK B., HAUSER H., LARAMEE R. S., DOLEISCH H.: The state of the art in flow visualisation: Feature extraction and tracking. *Computer Graphics Forum 22*, 4 (2003), 775–792. doi:10.1111/j.1467-8659.2003.00723.x. 2

[Rob09] ROBINSON M.: *Turbulence and Viscous Mixing using Smoothed Particle Hydrodynamics*. PhD thesis, Monash University, 2009. 2

[RTW13] REICHL F., TREIB M., WESTERMANN R.: Visualization of big SPH simulations via compressed octree grids. In *2013 IEEE International Conference on Big Data* (2013), IEEE, pp. 71–78. 2

[Sch02] SCHATZMANN M.: *Numerical Analysis: A Mathematical Introduction*. Oxford University Press, New York, USA, 2002. 2

[SFBP09] SCHINDLER B., FUCHS R., BIDDISCOMBE J., PEIKERT R.: Predictor-corrector schemes for visualization of smoothed particle hydrodynamics data. *IEEE Transactions on Visualization and Computer Graphics 15*, 6 (nov-dec 2009), 1243–1250. 2